Desalination and Water Treatment
www.deswater.com

doi:10.5004/dwt.2018.22531

125 (2018) 250–257
September

The performance study of eco-friendly alkali-activated oil shale cementing materials for wastewater treatment structure

Rui Ding[a], Lijun Chen[b], Yinshan Jiang[a,*]

[a]*Key Laboratory of Automobile Materials of Ministry of Education and Department of Materials Science and Engineering, Jilin University, Changchun, China, email: jiangyinshan@163.com (Y. Jiang)*
[b]*College of Material Science and Engineering, Jilin Jianzhu University,Changchun, China*

Received 3 March 2018; Accepted 17 May 2018

ABSTRACT

The oil shale residue (here after, OSR), as industrial waste residual by carbonization or burning of oil shale, can do damage to the environment. In this paper, a new kind of alkali-activated oil shale cement (AOC), with both high early strength and later strength has been developed by the application of composite water glass into slag-OSR system. The mortar was activated by less Na_2O (3.6 wt.%) which could reduce the production costs of AOC. The hydration products of this AOC mortars have been examined by means of XRD, DSC, FTIR, SEM, etc. The results indicated that the hardened AOC mortars were mostly consisted of C-S-H gel which being low in Ca/Si ratio. Unlike alkali-activated slag material, in the AOC mortars some zeolite-like products have been detected. The micro structures of AOC mortars had less porosity and the inter facial zone between aggregate and hydration products was dense and of homogeneous. By controlling the chemical composition of raw materials, it is possible to produce AOC mortar with mechanical strength comparable to conventional Portland cement mortars.

Keywords: Oil shale residue; Alkali-activated cement; Eco-friendly cementing materials; Wastewater treatment structure

1. Introduction

In existing engineering designs, chemistry corrosion on concrete structure in city wastewater treatment plant received little attention, though it happens widely in daily running systems, it is hard to find or care once the enclosed concrete structure completed. Developing with the city, the city wastewater treatment plant has been requested better function and higher standard, so the concrete chemistry corrosion problem should be emphasized [1–3].

Alkali-activated cement and concrete are new alternative building materials, whose main difference from traditional Portland cement concrete is the use of a relatively alkali-rich, clinker-free binder matrix. Compared with conventional concrete, the production of Alkali-cement and concrete are associated with low energy consumption, high corrosion resistance and low CO_2 emission, along with the potential to reach high mechanical strength and high stability [4–8].

Large number of fly ashes and other industrial wastes discharged by power station should have new applications, which could give a new impetus to Alkali-activated cement and concrete [9,10]. In the US, for example, 49% of the wastes from power station were returned to the landfills and 41% were emitted into settling basin.

In order to reduce the disposal expense, some industrial wastes were stacked up the ground that does not include the high-SO_3 wastes. However, there were few reports in the alkali activated based on other industrial waste residue, most of the research works were for Alkali-activated slag cement in the past. So the use of other industrial wastes for alkali activated cement has great excellent prospects.

*Corresponding author.

Presented at the 4th Annual Science and Technology Conference (Tesseract'17) at the School of Petroleum Technology, Pandit Deen Dayal Petroleum University, 10–12 November 2017, Gandhinagar, India

According to incomplete statistics, the oil shale resources are rich in the whole world and distribute in a broad range. There are about 10 trillion tons oil shale have been estimated which were 40% more than coal. Oil shale residue (OSR), a waste residual by carbonization or burning of oil shale, with high activity, would seriously pollute environment and occupy large area of useful land without rational reuse. However, there were few reports in the academic literature regarding alkali-activated cement and concrete based on oil shale waste, and the method to control chemical composition of alkali-activated cement and concrete has not been described. For the production of Portland cement caused a lot of environment and resources problems, the trend of cement industry should be aiming at producing alkali-activated cement and concrete by largely utilization of OSR, slag and flying ashes.

This work concentrated on alkali-activated oil shale cement (AOC) mortar activated by sodium silicate solution. The report also includes the producing methods and technical indexes of AOC mortar, which could make it reach the practical level and supply a new way for OSR recycling treatment technology, providing an effective control method of AOC production.

2. Experimental program

2.1. Materials

The raw materials used to produce the binder are OSR from the Huadian thermal power plants and granulated blast furnace slag form Tonghua steel plant, Jilin Province, China. The chemical composition of the granulated blast furnace slag and OSR used in this study are shown in Table 1. A pilot ball mill was used to prepare the slag and OSR with Blaine surface areas of 400 m^2/kg and 399 m^2/kg, respectively. The mineral composition of the OSR and slag are shown in Fig. 1, and the chemical composition of the OSR and slag are shown in Table 1.

The alkaline activation of the AOC was carried out using a sodium silicate solution ($Na_2O{\cdot}rSiO_2{\cdot}nH_2O$), with the silica modulus of the solution 1.2.

A commercial Portland cement clinker with Blaine fineness of 320 m^2/kg and specific gravity of 3300 kg/m^3 was used as adjusting setting agent and its chemical composition is shown in Table 1.

China standard sand was used as fine aggregates in the manufacture of AOC mortar. The specific gravity, absorption, and fineness modulus of the sand were 2400 kg/m^3, 3.75% and 2.4, respectively.

2.2. Experimental program

The binder/sand ratio of AOC mortars adopted here is of 1:3. The activating agents was water glass (SiO_2/Na_2O=1.2) with in which the Na_2O is 3.6 wt% of the binder. Portland cement clinker was added to all mixes as an adjusting setting agent at 4 wt% of the binder. The mixes were formulated to achieve mortar consistency of around 90 mm and a total water/binder ratio of 0.5. The specimens of AOC mortars (4×4×16 cm) were designed following the standard procedure GB/T 17671-1999, idt ISO 679: 1989 (Method of testing cements-Determination of strength), using same binder/sand and water/binder ratio specified for the AOC mortar. And the AOC mortar were kept in a humidity-controlled chamber (relative humidity of 95% RH) at 20 ± 2°C in order to prevent leaching of the alkaline activator, and the mix details are shown in Table 2.

2.3. Characterization

Compressive strength was evaluated from 1 to 90 d, the average of six specimens is reported. Fragments form mechanical testing were dried in vacuum at 105°C for 12 h to eliminate the free water available for the reaction. Samples of 3 d and 90 d were used for characterization by scanning electron microscopy (SEM). Futher more the hardened material was tested using a set of instrumental analytical methods to obtain mechanical, mineralogical, physical date at the multilevel. Methods included Fourier transform

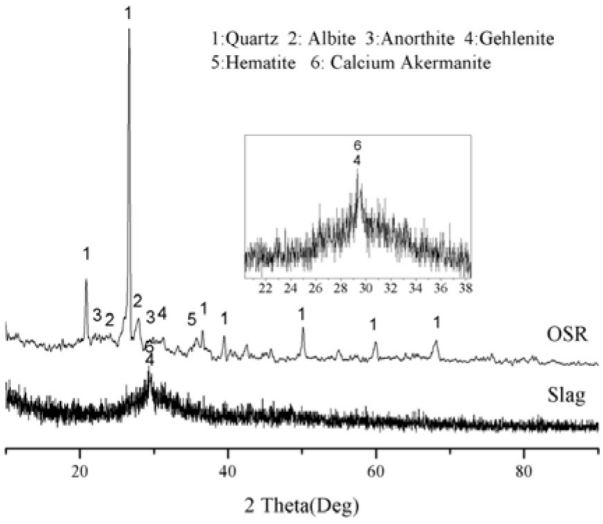

Fig. 1. Mineral composition of OSR and slag.

Table 1
Chemical composition of the starting materials

Item	Loss	SiO_2	Fe_2O_3	Al_2O_3	CaO	MgO	SO_3	K_2O	Na_2O
Oil shale residue (OSR)	2.55	2.85	7.73	16.30	5.10	1.43	0.88	2.00	1.01
Slag(S)	0.31	36.40	2.17	11.84	37.24	7.50	/	0.33	0.28
Portland cement clinker (adjustable setting-time agent)	/	21.75	4.00	4.62	65.81	1.15	0.47	0.51	0.25

infrared spectroscopy (FTIR), X-ray diffraction (XRD), and differential scanning calorimetry (DSC).

3. Results and discussion

3.1. Compressive and flexural strength

The development of mechanical strength of AOC mortar is given in Fig. 2. Compared with neat slag, higher compress and flexural strength can be observed while the mortar were 50% amount of OSR since the first day and up to 90 d of curing. It may be caused by that the OSR was performing as heterogeneous nucleation centers for the precipitation of the hydration products after the dissolution of the slag grains under the alkali action, and also accelerated the reaction speed. But the mechanical strength of AOC mortar was reduced when the OSR content exceeded 50%, the strength of 70% OSR was lower at all times. These results correlated well with the chemical composition of the OSR and slag. It has been known that the raw materials (except alkali-activator) of alkali-activated materials which can be divided into two categories: one is silicon-aluminum mineral, and the other is calcium-magnesium material or material containing silicon-aluminum and calcium-magnesium.

The OSR belongs to silicon-aluminum mineral, which is high in SiO_2 and Al_2O_3, low CaO and MgO content. By contrast, the slag which belongs to calcium-magnesium material has a high content of CaO and MgO. Therefore, Alkali-activated raw material consists of OSR and slag has a moderate Ca/Si ratio. For mortar with 50% OSR, the Ca/Si ratio of 0.45, higher than that used in a study of pozzolanic materials of 0.25 [11], it is possible to expect a pozzolanic behavior of the SiO_2 with the CaO, the OSR is also an activant to the slag. Many results indicate the higher that Ca/Si ratio the better breaking the Si-O bond and Al-O bond effect, but the higher Ca/Si need more alkali-activator. The alkaline activator was incorporated at a concentration of activation of 3.6% Na_2O in this paper which was lower than 7.5% Na_2O of other reports [12], therefore when the OSR was set as 70% (Ca/Si ratio of 0.29), the strength will be consequently lower according to less alkali-activator.

The high mechanical strength of AOC mortar is attributed to the physical and structural characteristics of the binders formed in these systems. Although the origin of the fast setting is not clear and more work is needed to elucidate it, but some possible mechanisms may be able to explain it, hydration reactions of AOC mortar are possibly affected by dissolution and precipitation phenomena, faster than the diffusion-controlled reaction process which take place in Portland cement hydration [13,14], therefore high compressive strength can be observed at the early age of curing. On the other hand, the amorphous OSR and slag go partly in solution of mixing cause the increases the viscosity and formed a gel, thought as a result of increased intermolecular forces due to neutralization of the charge or a kind of dehydration. Such as the alkali-activated slag material, the C-S-H (I) is one of the main hydration products in the AOC which has high later strength and excellent durability, during this alkali-activation reaction, the silicate ions which are both dissolved from the raw materials and supplied by water glass will react with the Ca^{2+} released from the slag and OSR. Condensation and cross-linking of these specimen leads to gelation, with some of the Si^{4+} substituted by Al^{3+} supplied by the OSR and slag, and others incorporating some alkalis into charge-balancing sites and sorbed onto

Table 2
Proportion of AOC mortars prepared with OSR and slag

Water/solids	0.5				
OSR (%)	0	40	50	60	70
Slag (%)	100	60	50	40	30
Na_2O (%) equivalent	3.6%	3.6%	3.6%	3.6%	3.6%
Portland cement clinker (adjustable setting-time agent)	4	4	4	4	4
Sand (g)	1350	1350	1350	1350	1350

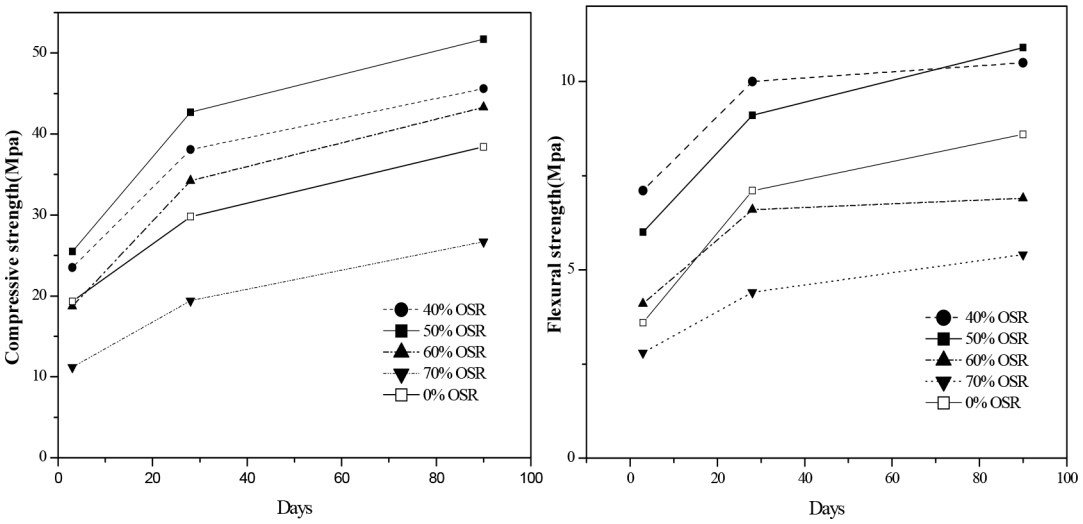

Fig. 2. Mechanical property of AOC mortar.

the gel structure, resulting in a calcium silicate hydrate type product with a low to moderate Ca/Si ratio [15–17].

And another hydration product which can be observed in the AOC mortar is aluminosilicate phases similar to the zeolite structure. In alkaline solution, OSR and slag were cracking into low polymerization degree silicon-oxygen tetrahedron and aluminum-oxygen tetrahedron similar to polymer monomer, and the polymerization of silicon oxygen tetrahedron and aluminum oxygen tetrahedron in alkaline environment subsequently formed three-dimensional netlike aluminosilicate [18]. However, the hydration products of Portland cement were mainly C-S-H gel formed by the hydrolysis and hardening of active silicate minerals, which nowadays was commonly recognized as a kind of inorganic polymer [19,20]. The essential distinction between these two hydration products was the diverse extent of polymerization in silicon oxygen tetrahedron and aluminum oxygen tetrahedron. The AOC mortar Ca/Si ratio adopted in this paper was much lower than the one (commonly 0.8–1.8) in C-S-H gel of Portland cement hydration products, thus under the same hydration condition, the extent of polymerization of the two tetrahedrons was relatively higher. And the SEM and XRD at later stage also proved that the hydration products of AOC mortars were mainly network structure formed by amorphous aluminosilicate containing a certain amount of C-S-H gel. The network structure of hydration products are believed to contribute positively to the development of higher mechanical strengths at advanced age of curing, and also have better durability than Portland cement.

3.2. Micro structures and microanalysis

It was shown the formation and evolution of OSR micro structure activated by water glass in Fig. 3. In the first 2 h, the micro structure feature of the AOC mortar was quite similar to the alkali-activated slag cement, with the OSR and slag surface-corroded and partial reaction product deposited. On the 1st day, most grains of OSR and slag were covered by hydration products, with no connection among these grains. Even though the hydration products gets in compact structure, the characteristics of OSR and slag particle outline are difficult to identify, and the remarkable feature of hydration products can only been observed in the voids.

The AOC mortar micro structure of hydration products is shown in Fig. 4. In the presence of 50% OSR, the matrix of hydration products appeared more compact than the others. It seems that the appropriate OSR content seemed to have better effect to improved compactness of the matrix as well as the strength. As the hydration time grows, the section structure of the AOC mortar is to have better compactness, among which can be observed the flocculated particles and a few hexagonal hydration products. All the specimens is highly amorphous, the crystalline phases originate from residual and sparingly soluble parts of raw materials, namely zeolite and quartz. The hexagonal hydration products could be C-S-H gel, showing laminate structure C-S-H adopted in Fig. 3, in contrast to C-S-H with higher Ca/Si ratio in Portland cement which was more like fiber-shaped. When OSR is blended with slag, clinker-like hydrated phases will coexist with C-S-H in the matrix of AOC. Recent experimental results pointed higher compressive strength when C-S-H coexisted in the matrix.

The micro structures of AOC mortar in Fig. 4 show the interface between the sand and the hydration products was still dense and compact after 90 d, within which can be observed chemical reactions, in contrast to the porous zone and inter facial transition zone reported for Portland cement mortars.

In Fig. 5, as the OSR content is of 50%, the interface between sand and hydration product showed fine compactness after 90 days of curing, and no crystal products were observed such as $Ca(OH)_2$, in contrast to the heterogeneous inter facial transition zone in Portland cement mortars. In conclusion, the SEM investigation on the micro structure of AOC mortar with 50% OSR addition gave a reasonable answer to its higher mechanical strength mentioned in section 3.1.

3.3. X-ray diffraction (XRD)

Fig. 6 shows the result of XRD analysis on the hardened AOC mortar, which at the least revealed something as follows:

All the XRD patterns show that the similar features. Therefore, the similar composition and almost the same hydration products regardless of the change of OSR and slag content, indicated that all the crystallized minerals in the

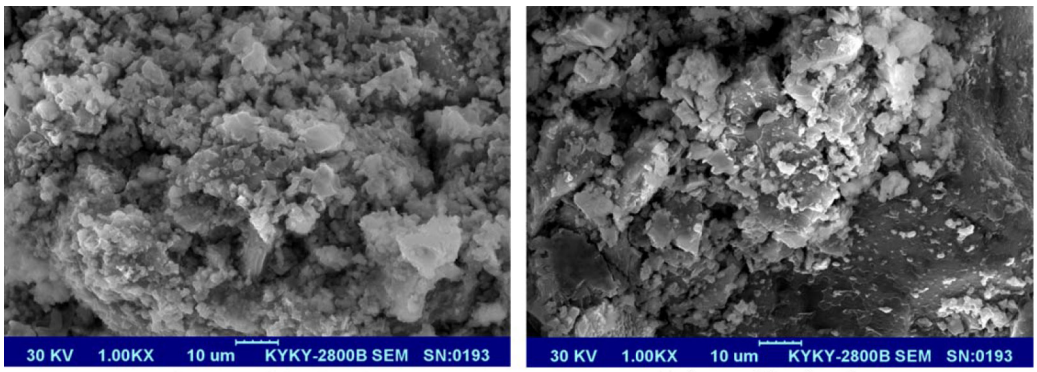

Fig. 3. The Formation process of the AOC mortar (50% OSR) micro structure.

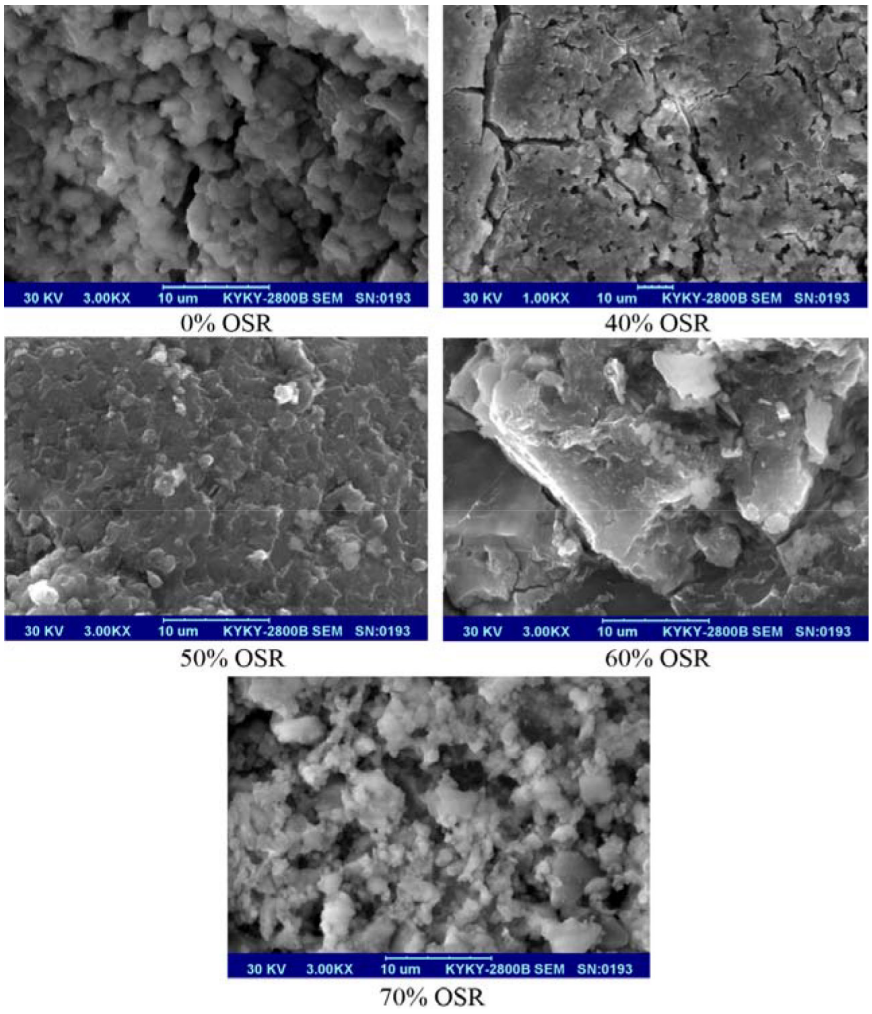

Fig. 4. The micro structure of hydration products.

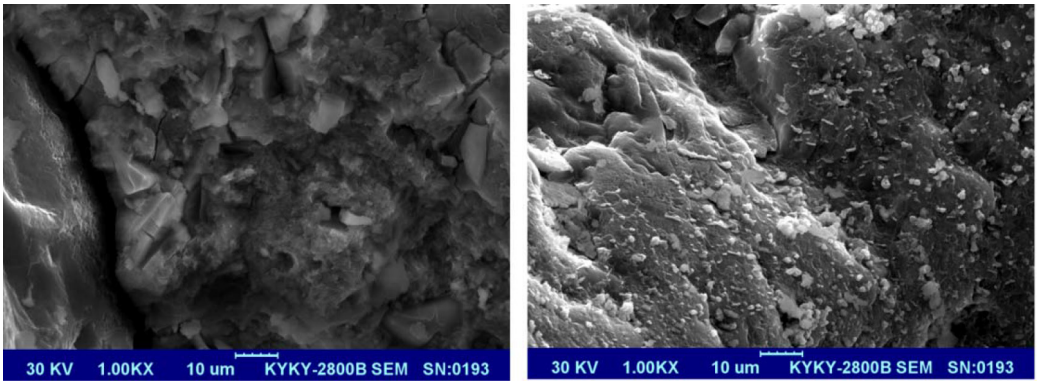

Fig. 5. SEM of the interface between sand and hydration product (50% OSR).

hardened cement paste system come from raw materials, along with some new amorphous hydration products were formed.

As we can see in the XRD pattern, the hardened AOC mortar contains lots of α-quartz (mainly from raw materials), along with certain amount of Sodilium Aluminosilicate hydrate ($Na_4Al_2Si_6O_{17}\cdot 2H_2O$), unnamed Zeolite ($Na_2O$-$Al_2O_3$-$SiO_2$-$H_2O$) and a small number of C-S-H gels, etc. With the OSR content increasing, the diffraction peak value of α-SiO_2 in the AOC mortar was growing gradually, which reflected lower hydration degree of OSR and slag and reduced reaction degree of SiO_2. On the contrary, the diffraction peak value of

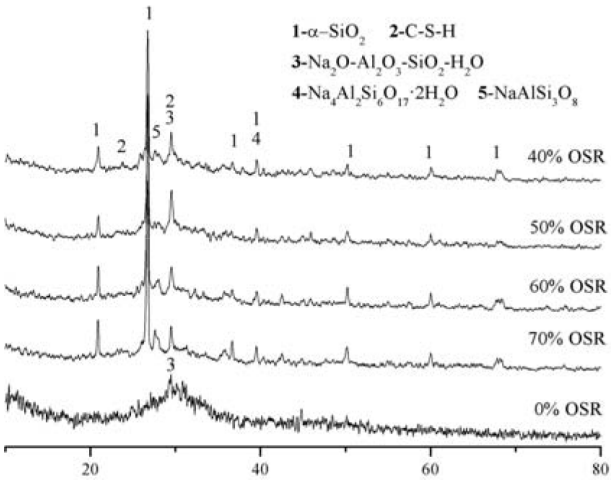

Fig. 6. Result of XRD analysis of hardened AOC mortar.

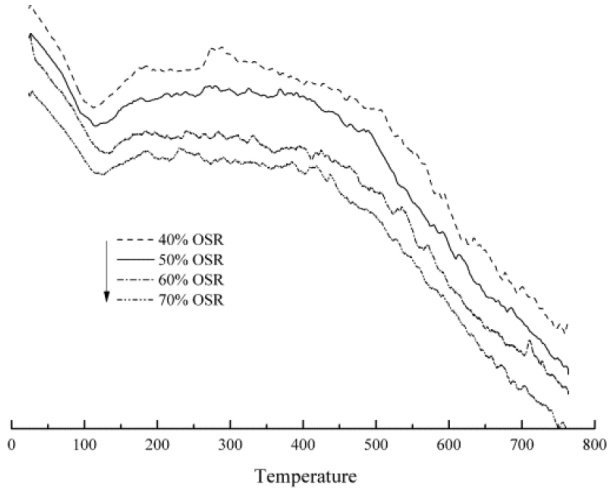

Fig. 7. DSC analysis of the hardened AOC mortar.

C-S-H and Na_2O-Al_2O_3-SiO_2-H_2O was reducing by degrees, it proved that when OSR content is proper (50% OSR), the hydration degree of raw material was comparatively higher under the effect of activator, which would produce more C-S-H and amorphous Na_2O-Al_2O_3-SiO_2-H_2O, this progress is perfectly fit to the mechanical strength curve .

3.4. DSC analysis

Results of DSC analysis on AOC hardened specimen cured at ambient temperature are shown in Fig. 7, which show the similar features as those of hardened Portland cement paste system except for the additional exothermic effect between 200 and 600°C probably being caused by the dehydration of C-S-H. The floating of the base line of the DSC curves implies the existence of large amount of C-S-H gel, that is for water in different bonding status in C-S-H gel structure has different bonding energy. The endothermic effect at around 120°C may be due to the discharge of absorbed water in capillary pores in the hardened AOC paste.

It is appropriate to emphasize that no endothermic effect around 450°C, which was normally caused by the dehydration of $Ca(OH)_2$, was detected, that indicated no $Ca(OH)_2$ formed in hardened AOC mortar. This result is in a very good agreement with that obtained by XRD analysis.

3.5. FTIR analysis

The FTIR analysis of hardened AOC mortar specimens is shown in Fig. 8, within which the wide absorption band in wave length 3500 cm^{-1} to 3400 cm^{-1} was due to C-S-H gel, as the addition of OSR reached 50%, the absorption band was at its most, and proved that more C-S-H gels were produced. The absorption band in wave number 1000 cm^{-1} to 1500 cm^{-1} was due to the polymerization degree change of reaction products, which was shown in the FTIR fig as that the absorption band of the stretching vibration of Si-O-T (T=Si or Al) shifted to lower wave number, additionally, this shifting can also be triggered when some $[SiO_4]^{4-}$ group in silicon-oxygen tetrahedron were replaced by aluminum-oxygen tetrahedron. As we can see in the Fig. 6, when the OSR

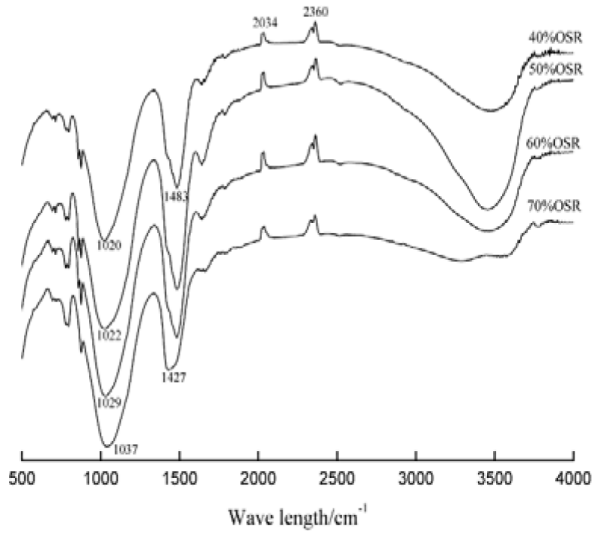

Fig. 8. IR analysis of the hardened AOC mortar.

amount increased, the absorption band of Si-O-T shifted to higher wave number, which indicated that the silicon-oxygen tetrahedron and aluminum-oxygen tetrahedron from AOC mortar suffered a loss in polymerization degree. In addition, the absorption band at 1500 cm^{-1} was belong to the flexural vibration and stretching vibration of O-H in bound water, and the upward peak showed in 2000 cm^{-1} and 2500 cm^{-1} were caused by the disturbance from CO_2 and H_2O in FTIR chamber.

3.6. TEM analysis

C-S-H is composed of nano-colloidal particles, so the use of TEM at high resolution can give better view of its morphological structure than the SEM. In our study, TEM was used to investigate the AOC mortar of 50% content OSR, and the test result is shown in Fig. 9. As we can see in Figs. 9a and b by 20 nm scale observation, the hydration products is a kind of agglomeration consisted of irregular

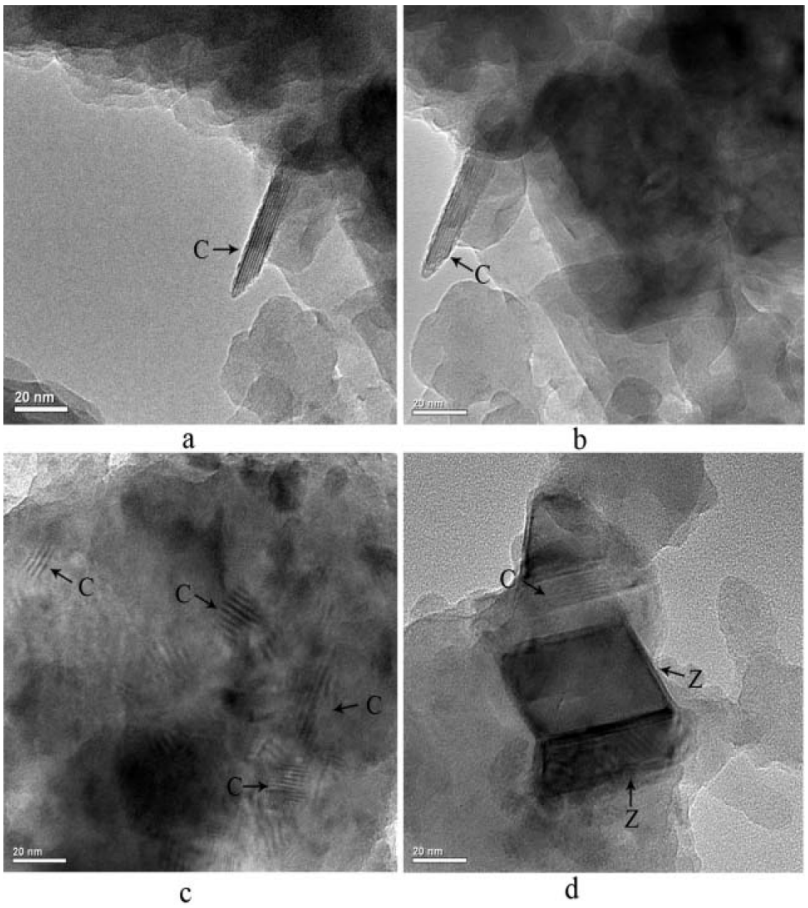

Fig. 9. TEM analysis of the hardened AOC mortar.

forms particles and sheet-like object, within which the distinct layered structure can be clearly identified as C-S-H gel, same to the result confirmed by other paper [20].

In Fig. 9, the lower resolution was caused by the thickness in middle part which reduced the penetration power of electron beam, but still could we identify the C-S-H layered structure. In Fig. 9d, the sheet-like object observed is a kind of zeolite-like product consisting of sodilium aluminosilicate ($Na_4Al_2Si_6O_{17}\cdot 2H_2O$) and unnamed zeolite ($Na_2O$-$Al_2O_3$-$SiO_2$-$H_2O$), this zeolite-like product together with C-S-H formed a net like space structure, which was also proved by results of XRD, IR and DSC tests.

4. Conclusion

The study of OSR is a help for recycling specific heterogeneous hazardous waste material containing high amount of SiO_2 and Al_2O_3. Performed analyses lead to following conclusions.

1. By analysis of AOC mortar prepared at a range of OSR and slag, using alkali-activated oil shale cement as binder materials, the effects of mortar mix experiment on mechanical and hydration products have been determined. For 50% OSR contents, the AOC mortars with lower alkali-activator generate higher strengths at both 28 and 90 d. This was caused by the network structure formed by amorphous aluminosilicate containing a certain amount of C-S-H gel.
2. The SEM images showed that the interface of hydration products with the sand was dense and compact in the systems. The microanalysis of the hydration products in AOC mortar indicated that in low Ca/Si ratio condition, C-S-H gel was formed and intermixed with zeolite-like product, which was confirmed by XRD.
3. Alkali-activated cement prepared by alkali-activated oil shale is a new family of inorganic binders originating from waste materials, whose mechanical properties are comparable with cementitious materials with superior chemical resistance, and highly favorable to the environmental.

Acknowledgements

This work is financially supported by the National Natural Sciences Foundation of China (Grant No. 41072025 and 41472035) and The science and technology research project of Jilin Province Education Department(Grant No. 2017102).

References

[1] M. Sogancioglu, E. Yel, S. Aksoy, V.E. Unal, Enhancement of concrete properties by waste physico chemical treatment sludge of travertine processing wastewater, J. Cleaner Product., 112(1) (2016) 575–576.

[2] W. Ben, B. Zhu, X.j. Yuan, Y. Zhang, M. Yang, Z. Qiang, Occurrence, removal and risk of organic micro pollutants in wastewater treatment plants across China: Comparison of wastewater treatment processes, Water Res., 130(1) (2018) 38–39.

[3] K.M. Liew, A.O. Sojobia, L.W. Zhang, Green concrete: Prospects and challenges, Constr. Build. Mater., 156(15) (2017) 1063–1090.

[4] S.A. Bernal, Effect of binder content on the performance of alkali-activated slag concretes, Cem. Concr. Res., 41 (2017) 1–8.

[5] D. Roy, Alkali-activated cements-opportunities and challenges, Cem. Concr. Res., 29(2) (1999) 249–254.

[6] R. Tänzera, Y. Jin, D. Stephan, Effect of the inherent alkalis of alkali activated slag on the risk of alkali silica reaction, Cem. Concr. Res., 98(1) (2017) 82–84.

[7] M. Mun, H. Cho, Mineral carbonation for carbon sequestration with industrial waste, Energy Procedia., 31(1) (2013) 6999–7002.

[8] S.-D. Wang, X.-C. Pu, K.L. Scrivener, P.L. Pratt, Alkali-activated slag cement and concrete: a review of properties and problems, Adv. Cem. Res., 7(27) (1995) 93–102.

[9] T. Luukkonen, Z. Abdollahnejad, J. Yliniemi, M. Illikainen, One-part alkali-activated materials: A review, Cem. Concr. Res., 103 (2018) 21–34.

[10] F. Fan, Z. Liu, G. Xu, H. Peng, C.S. Cai, Mechanical and thermal properties of fly ash based geopolymers, Constr. Build. Mater., 160(30) (2018) 66–70.

[11] C. Shi, R.L. Day, Pozzolanic reaction in the presence of chemical activators: Part I. Reaction kinetics, Cem. Concr. Res., 30 (2000) 51–58.

[12] F. Skvára, L. Kopecký, V. Smilauer, Z. Bittnar, Material and structural characterization of alkali activated low-calcium brown coal fly ash, J. Hazard. Mater., 168(1) (2009) 711–720.

[13] D.M. Roy, M.R. Silsbee, Alkali activated materials. An overview, Mater. Res. Soc. Symp. Proc., 245 (1992) 153–164.

[14] S.-D. Wang, K.L. Scrivener, Hydration products of alkali-activated slag cement, Cem. Concr. Res., 25(3) (1995) 561–571.

[15] A. Fernández-Jiménez, F. Puertas, Structure of calcium silicate hydrates formed in alkaline-activated slag: influence of the type of alkaline activator, J. Am. Ceram. Soc., 86(8) (2003) 1389–1394.

[16] S.-D. Wang, K.L. Scrivener, 29Si and 27Al NMR study of alkali-activated slag, Cem. Concr. Res., 33(5) (2003) 769–774.

[17] E. Papa, V. Medri, S. Amari, J. Manaud, P. Benito, A. Vaccari, E. Landi, Zeolite-geopolymer composite materials: Production and characterization, J. Cleaner Product, 171(10) (2018) 78–82.

[18] J. Davidovits, Geopolymers: man-made rock geosynthesis and the resulting development of very early high strength cement, J. Mater. Educ., 16(2,3) (1994) 91–139.

[19] D. Stephan, R. Tänzer, T. Braun, M.S. Prof. Dr.-Ing. Habil, H.M. Schmidt, Alkali activation an alternative to binders that contain clinker; part1 and part2, Cement Int., 1(8) (2010) 73–85 and 2(8) (2010) 75–81.

[20] A. Gmira, R.J.-M. Pellenq, I. Rannou, L. Duclaux, C. Clinard, T. Cacciaguerra, N. Lequeux, H. Van Damme, A structural study of dehydration/rehydration of tobermorite, a model cement compound, Studi. Surf. Sci. Catal., 144 (2002) 601–608.